Minimal Impact Corrective Actions in Security-Constrained Optimal Power Flow Via Sparsity Regularization

Dzung T. Phan and Xu Andy Sun, *Member, IEEE*

***Abstract*—This paper proposes a new formulation for the corrective security-constrained optimal power flow (SCOPF) problem with DC power flow constraints. The goal is to produce a generation schedule which has a minimal *number* of post-contingency corrections as well as a minimal *amount* of total MW rescheduled. In other words, the new SCOPF model effectively clears contingencies with corrective actions that have a *minimal impact* on system operations. The proposed SCOPF model utilizes sparse optimization techniques to achieve computational tractability for large-scale power systems. We also propose two efficient decomposition algorithms. Extensive computational experiments show the advantage of the proposed model and algorithms on several standard IEEE test systems and large-scale real-world power systems.**

***Index Terms*—Decomposition algorithm, ℓ_1 regularization, security-constrained optimal power flow.**

I. Introduction

CONTINGENCY analysis is routinely performed in the operation of power systems. The goal is to ensure that the system remains balanced and reliable in both normal state and contingencies when any one or more components in the power system, such as generators, transmission lines, transformers, or other equipments, experience unexpected failure. The optimal power flow (OPF) problem with contingency constraints considering the failure of one component at a time is often referred to as the $N-1$ security-constrained optimal power flow (SCOPF). There are two major types of SCOPF models: the preventive model [2] and the corrective model [32].

The preventive SCOPF model (denoted as P-SCOPF) finds a minimum cost normal state dispatch solution that is also feasible for all pre-specified contingency conditions. A general formulation is given as follows:

$$\min_{\boldsymbol{u}_0,\boldsymbol{x}_c,\forall c\in\{0\}\cup\mathcal{C}} \quad f(\boldsymbol{x}_0,\boldsymbol{u}_0) \tag{1a}$$

$$\text{s.t.} \quad \boldsymbol{g}_c(\boldsymbol{x}_c,\boldsymbol{u}_0)=\boldsymbol{0}, \quad c\in\{0\}\cup\mathcal{C} \tag{1b}$$

$$\boldsymbol{h}_c(\boldsymbol{x}_c,\boldsymbol{u}_0)\le\boldsymbol{0}, \quad c\in\{0\}\cup\mathcal{C} \tag{1c}$$

where $\boldsymbol{x}_0$ and $\boldsymbol{x}_c$ represent state variables, such as nodal voltages, of the normal state $c=0$ and the cth contingency, respectively; $\mathcal{C}=\{1,2,\ldots,C\}$ is the index set of pre-specified C contingencies; in the following, we denote $\overline{\mathcal{C}}=\{0\}\cup\mathcal{C}$; $\boldsymbol{u}_0$ represents control variables, such as generators power output, of the normal state; (1a) is the normal state cost; (1b) represents flow balance equations, and (1c) represents physical limit constraints on the generation output levels and circuit power flow. In this paper, we are interested in transmission line contingencies. So the cth contingency corresponds to the failure of the cth transmission line. As noted above, the preventive model requires the normal-state control variable $\boldsymbol{u}_0$ to be feasible for all contingency constraints.

The second type of SCOPF model is the so-called corrective model (denoted as C-SCOPF), which allows the system operator to re-adjust control variables after a contingency occurs. The rationale is that the electrical components in the power system, such as transmission lines and transformers, can usually sustain a short period of overloading without being damaged [32]. This capability gives the system operator a time window to adjust control variables in order to eliminate any violations caused by the contingency. Using the same notation, the C-SCOPF can be formulated as follows:

$$\min_{\boldsymbol{x}_c,\boldsymbol{u}_c,\forall c\in\{0\}\cup\mathcal{C}} \quad f(\boldsymbol{x}_0,\boldsymbol{u}_0) \tag{2a}$$

$$\text{s.t.} \quad \boldsymbol{g}_c(\boldsymbol{x}_c,\boldsymbol{u}_c)=\boldsymbol{0}, \quad c\in\overline{\mathcal{C}} \tag{2b}$$

$$\boldsymbol{h}_c(\boldsymbol{x}_c,\boldsymbol{u}_c)\le\boldsymbol{0}, \quad c\in\overline{\mathcal{C}} \tag{2c}$$

$$|\boldsymbol{u}_c-\boldsymbol{u}_0|\le\bar{\boldsymbol{u}}_c^{\max}, \quad c\in\mathcal{C}. \tag{2d}$$

Here, the system operator minimizes the normal state cost (2a), but now it has the flexibility to choose a control variable $\boldsymbol{u}_c$ for each contingency c in (2b) and (2c). The last constraint (2d) imposes that the deviation between the normal state and

Manuscript received February 22, 2014; revised June 04, 2014 and August 01, 2014; accepted August 06, 2014. Date of publication October 08, 2014; date of current version June 16, 2015. This work was supported in part by the National Science Foundation [Award CCF1331426]. Paper no. TPWRS-00257-2014.

D. T. Phan is with the Mathematical Sciences Department, IBM T. J. Watson Research Center, Yorktown Heights, NY 10598 USA (e-mail: phandu@us.ibm.com).

X. A. Sun is with the H. Milton Stewart School of Industrial and Systems Engineering, Georgia Institute of Technology, Atlanta, GA 30332 USA (e-mail: andy.sun@isye.gatech.edu).

Color versions of one or more of the figures in this paper are available online at http://ieeexplore.ieee.org.

Digital Object Identifier 10.1109/TPWRS.2014.2357713

the post-contingency controls for each contingency c must be within the bound $\bar{\boldsymbol{u}}_c^{\max}$. Note that constraints (2d) should be understood componentwise as $|u_{c,i} - u_{0,i}| \le \bar{u}_{c,i}^{\max}, \forall i$.

The P-SCOPF model (1) forsakes the option to adjust control variables, which makes the solution intrinsically conservative and may result in a high operating cost. The situation can be even worse for the preventive model when a feasible operating point satisfying both normal and contingency constraints does not exist. In comparison, the C-SCOPF model (2) is more flexible in terms of allowing adjustment to control variable values and thus may achieve a lower operating cost. However, the C-SCOPF model also has some difficulties.

1) The first difficulty is computational, which is, to some degree, shared by both preventive and corrective models. In particular, SCOPF models have huge dimensionality. For C contingency scenarios, the P-SCOPF model has the same number of control variables and $C + 1$ times more state variables and constraints compared to the normal state OPF model; the C-SCOPF model has roughly $C + 1$ times more state and control variables and constraints than the normal state OPF. For large-scale power systems involving numerous contingencies, centralized solution algorithms may encounter prohibitive issues such as memory limit and long computation time.
2) The second difficulty, unique to C-SCOPF, is that the optimal solution of the corrective model usually requires to adjust the output levels of a large number of generators (see discussions in [9], [10], [12], and [30]). This property is particularly undesirable in the current industry practice for several reasons. First, the system operators may only be able to handle a limited number of corrective actions due to time and communication constraints. Second, even if the system operator is capable of handling all corrective actions, from a security perspective, it is much more reliable to clear the contingency via adjusting a few number of generators.
3) The third difficulty, also unique to C-SCOPF, is that the corrective actions in the C-SCOPF model may involve a large amount of MW rescheduling between the normal state and contingencies. This will be demonstrated in computational experiments in this paper. A large amount of MW rescheduling not only increases operational complexity and reduces system security, but also induces high cycling costs to generators [27].

To deal with the first computational difficulty, several approaches are proposed in the literature. The main approaches include iterative contingency selection schemes [1], [3], [5], [8], [20], where contingency filtering techniques are developed to identify and include only those potentially binding contingencies into the formulation; decomposition methods [29], [32], [35], [38], where Benders decomposition is used to decompose the SCOPF into a master problem and subproblems, which check the solution feasibility and generate linear cuts to the master problem; and a network compression method [26], which is based on the observation that the impact of a contingency is in general confined to a localized area of the power grid.

The second difficulty specific to the C-SCOPF model attracts much attention recently. A series of papers [9], [10], [12], [13], [30] discussed and proposed new models and solution methods to resolve this issue. One of the key proposals is to use the following constraints to limit the number of corrective actions:

$$|u_{c,i} - u_{0,i}| \le \bar{u}_{c,i}^{\max} s_{c,i} \quad \forall i \in \mathcal{G}, c \in \mathcal{C} \tag{3a}$$

$$\sum_{i \in \mathcal{G}} s_{c,i} \le N_c, \quad s_{c,i} \in \{0,1\} \quad \forall i \in \mathcal{G}, c \in \mathcal{C} \tag{3b}$$

where $\mathcal{G}$ is the set of generators, N_c is the maximum number of corrective actions allowed, and binary variable $s_{c,i} = 1$ if generator i's output can be changed in the cth contingency. Constraint (3a) limits the output deviations of generators that are allowed to change in each contingency c. In the optimal solution, constraint (3b) is usually satisfied as equality, i.e., the number of changes would be equal to the maximum number N_c, which is selected before the operation of the system.

The proposed constraint (3) allows the system operator to control the number of corrective actions needed to clear the contingency. However, it also has some drawbacks. The foremost one is that contraint (3) requires binary variables in the C-SCOPF formulation, which significantly increases the computational complexity of the resulting model. The recent paper [30] proposed a method to exploit the use of DC SCOPF approximation to improve the iterative AC SCOPF algorithms. Although this approach effectively reduces the complexity of solving the AC SCOPF model, the proposed DC SCOPF approximation still contains binary variables, which makes it a mixed-integer program (MIP) rather than the efficient continuous formulation of the traditional DC SCOPF. Secondly, for a large-scale power system, selecting a proper N_c, the number of needed post-contingency actions, to ensure feasibility of the resulting corrective SCOPF is not a trivial task. Pre-setting the value of N_c may require some trial and error, which can be time consuming and situation dependent.

The third difficulty specific to the C-SCOPF model does not seem to have been much studied in the literature. We conduct extensive computational experiments on several IEEE test systems of small (39-bus), medium (118-bus and 300-bus), and large-scale (2383-bus and 3012-bus) sizes. The results show that, for the conventional C-SCOPF model (2), the average absolute value of the total MW rescheduling between the normal state and a contingency state is around 3.15%–9.68% of the total load, which leads to a large amount of cycling (i.e., ramping up and down) of generators. Proposal (3) restricts the total *number* of rescheduling, and its effect on reducing the *amount* of MW rescheduling is neither direct nor optimized.

The above considerations motivate us to pursue a new corrective SCOPF model to achieve the goal of producing a generation schedule which has a minimal *number* of post-contingency corrections as well as a minimal *amount* of total MW rescheduled in corrective actions. In other words, the new

SCOPF model effectively clears contingencies with corrective actions that have a *minimal impact* on system operations. The new model should also be computationally efficient by avoiding integer decision variables, easy to decompose and viable for parallel or distributed computation, and situation optimal in the sense that the proposed C-SCOPF model lets the optimization itself determine the best number of post-contingency actions based on the system operating condition when the contingency occurs, rather than pre-specify a fixed number.

The key observation is that the number of post-contingency rescheduling for contingency c is the same as the number of non-zero entries in the vector $(\boldsymbol{u}_c - \boldsymbol{u}_0)$. A vector with only a few number of non-zero entries is called a *sparse* vector. Therefore, the task of finding a generation schedule with few post-contingency reschedulings is equivalent to finding $\boldsymbol{u}_0$ and $\{\boldsymbol{u}_c\}_{c\in\mathcal{C}}$ such that the resulting $(\boldsymbol{u}_c - \boldsymbol{u}_0)$ is a sparse vector for each $c \in \mathcal{C}$. Furthermore, to find a corrective action that has a minimal amount of MW rescheduling is equivalent to minimizing a certain distance between $\boldsymbol{u}_0$ and $\boldsymbol{u}_c$. These two objectives, namely inducing a sparse solution as well as producing a small total deviation, can be unified by sparse optimization techniques.

With this motivation, we may summarize the main contributions of the paper as follows:

1) We propose a new type of C-SCOPF model, which we call *min-impact C-SCOPF*. It utilizes sparse optimization techniques to induce solutions of sparsity and small MW variations in post-contingency corrections, and it does not require any binary or integer variables. For DC power flow models, the proposed C-SCOPF formulation is again a convex program, which can be much more efficiently solved than models involving constraints (3).
2) The paper introduces efficient decomposition methods based on the alternating direction method of multipliers (ADMM) and its accelerated version [6], [23]. Using these methods, the min-impact C-SCOPF model is decomposed into a master problem and subproblems, each corresponding to a contingency. These subproblems are independent of each other, and can be solved by distributed and parallel computation. The decomposition scheme is also easy to implement.
3) We conduct extensive computational experiments on standard IEEE test systems and real-world sized power systems. The computational results show that the min-impact C-SCOPF model effectively reduces the number of post-contingency actions and simultaneously achieves essentially the same operational cost as the traditional corrective SCOPF model. The proposed decomposition methods also significantly outperforms existing methods with the state-of-the-art solvers.

In this paper, we focus on using DC power flow models in the OPF problem. Despite of many excellent studies (see, e.g., [8], [11], [22], [31], [32], [35], [37], and [40]), solving SCOPF problems with AC power flow constraints is still a major computational challenge in power system analysis. At the same time, SCOPF with DC power flows is widely used in the industry practice. Many ISOs in the U.S. are using linearization in one form or another to approximate the full AC OPF in their day-ahead and real-time operations [14], [38]. A similar observation is also reported in a recent comprehensive overview of the current industry practice in real-time operation and planning, published by FERC [21]. Based on these reports and our own interactions with the practitioners, improvements on DC SCOPF models will have significant impact on the industry. In fact, solving DC SCOPF models reliably and quickly for large-scale power systems is still a computational challenge. Some recent works show promising results in this direction [3], [15], [30], [38]. As a step toward obtaining solutions feasible to the AC power flow model, an AC feasibility check module can be coupled to the DC SCOPF model in an iterative manner. Recent work such as [30] has made notable progress in exploiting DC SCOPF approximation to solve the AC SCOPF problem, which is also the ultimate goal of this research. However, to emphasize the key innovation of the paper, we keep the presentation with DC power flows.

The organization of the paper is as follows. Section II proposes the new corrective SCOPF model. Section III introduces efficient decomposition algorithms to solve the proposed model. Section IV reports computational results. Section V concludes the paper.

II. Min-Impact C-SCOPF

We propose the following DC-based min-impact C-SCOPF model to achieve significant reduction in the number of post-contingency actions and the amount of MW rescheduling:

$$\min_{\{\boldsymbol{p}^c,\boldsymbol{\theta}^c\}_{c\in\overline{\mathcal{C}}}} \quad f(\boldsymbol{p}^0) + \tau \sum_{c\in\mathcal{C}} \left\|\boldsymbol{p}^c - \boldsymbol{p}^0\right\|_1 \tag{4a}$$

$$\text{s.t.} \quad F^c(\boldsymbol{p}^c, \boldsymbol{\theta}^c, \boldsymbol{d},) \le \boldsymbol{0}, \quad \forall c \in \overline{\mathcal{C}} \tag{4b}$$

$$\underline{\boldsymbol{p}} \le \boldsymbol{p}^c \le \bar{\boldsymbol{p}}, \quad \forall c \in \overline{\mathcal{C}} \tag{4c}$$

$$\underline{\boldsymbol{\theta}} \le \boldsymbol{\theta}^c \le \bar{\boldsymbol{\theta}}, \quad \forall c \in \overline{\mathcal{C}} \tag{4d}$$

$$|\boldsymbol{p}^c - \boldsymbol{p}^0| \le \Delta\boldsymbol{p}, \quad \forall c \in \mathcal{C} \tag{4e}$$

where the decision variables are power output of generating units $\boldsymbol{p}^0$ and bus voltage angles $\boldsymbol{\theta}^0$ for the normal state, and $\boldsymbol{p}^c, \boldsymbol{\theta}^c$ for each contingency c in the contingency index set $\mathcal{C}$. The constraints (4b)–(4e) are standard in DC-based C-SCOPF models. In particular, (4b) includes the power flow balance and flow limit constraints for the transmission network in contingency c when the cth transmission line is outed (equalities can always be expressed by two opposing inequalities); (4c) and (4d) are bound constraints on the generators' output levels and the bus voltage angles, respectively; (4e) constrains the difference between the normal state and post-contingency generation levels, where $\Delta\boldsymbol{p}$ depends on the generators' ramping capabilities.

A. Sparsity and ℓ_1-Regularization

The key deviation of the proposed model (4) from the existing C-SCOPF model (2) is in the objective function (4a), which has the following additional term:

$$\tau \sum_{c\in\mathcal{C}} \|\boldsymbol{p}^c - \boldsymbol{p}^0\|_1 = \tau \sum_{c\in\mathcal{C}} \sum_{i\in\mathcal{G}} |p_i^c - p_0^c| \tag{5}$$

with $\tau > 0$. This term is called the ℓ_1-regularization, which is added exactly for the purpose of inducing sparsity in $(\boldsymbol{p}^c - \boldsymbol{p}^0)$.

The technique of ℓ_1-regularization has become very influential in the compressed sensing community (e.g., see [7], [17], and [19]). As an example, let us consider a classical problem in signal processing, called the sparse signal recovery. In particular, we want to find a solution $\boldsymbol{x}$ to the linear system $\boldsymbol{M}\boldsymbol{x} = \boldsymbol{b}$ so that $\boldsymbol{x}$ has the least number of nonzero entries, i.e., the sparsest solution. This problem can be formulated as $\min\{\|\boldsymbol{x}\|_0 : \boldsymbol{M}\boldsymbol{x} = \boldsymbol{b}\}$, where the ℓ_0-norm $\|\boldsymbol{x}\|_0$ simply counts the number of nonzero entries in $\boldsymbol{x}$. However, $\|\boldsymbol{x}\|_0$ is a non-convex function and directly minimizing this function over linear constraints is proved to be an NP-hard problem [33]. It can be reformulated by introducing integer variables, which then lead to a mixed-integer program. To avoid the computational burden of solving MIPs, we can approximate $\|\boldsymbol{x}\|_0$ by a convex function. It turns out that the *tightest* convex approximation to $\|\boldsymbol{x}\|_0$ on the hypercube $[-1, 1]^n$ is the ℓ_1-norm $\|\boldsymbol{x}\|_1$ (see, e.g., [18].) Therefore, $\min\{\|\boldsymbol{x}\|_1 : \boldsymbol{M}\boldsymbol{x} = \boldsymbol{d}\}$ represents a convex approximation to the difficult problem of sparse signal recovery. In fact, in many situations, the ℓ_1-norm minimization recovers the exact sparse solution. The amazing effectiveness of the ℓ_1-regularization is observed in a wide range of applications in signal processing (e.g., see [4], [28], and [39]). This powerful sparse optimization technique seems to just start finding its applications in power system analysis. Jabr *et al.* [25] is among the first to use the ℓ_1-norm to minimize the amount of reactive power injection and the number of locations installed for VAr planning under various operating scenarios.

For our problem of C-SCOPF, the ℓ_1-regularization term in (5) "kills two birds with one stone" in the sense that it not only induces sparisty in $(\boldsymbol{p}^0 - \boldsymbol{p}^c)$, but also minimizes the absolute value of total variations between the normal state and the post-contingency solutions.

B. Reformulation to a Smooth Optimization Problem

Note that the min-impact C-SCOPF model (4a)–(4e) is a non-smooth convex optimization problem due to the non-smoothness of the ℓ_1-norm term, which makes it difficult to solve directly. However, (4a)–(4e) can be reformulated as a smooth optimization problem by using new variables w_i^c:

$$\min \quad f(\boldsymbol{p}^0) + \tau \sum_{i\in\mathcal{G},c\in\mathcal{C}} w_i^c \tag{6a}$$

$$\text{s.t.} \quad (\boldsymbol{p}^c, \boldsymbol{\theta}^c) \in \mathcal{F}_c \quad \forall c \in \overline{\mathcal{C}} \tag{6b}$$

$$-\Delta\boldsymbol{p} \le \boldsymbol{p}^c - \boldsymbol{p}^0 \le \Delta\boldsymbol{p} \quad \forall c \in \mathcal{C} \tag{6c}$$

$$-\boldsymbol{w}^c \le \boldsymbol{p}^c - \boldsymbol{p}^0 \le \boldsymbol{w}^c \quad \forall c \in \mathcal{C} \tag{6d}$$

where $\mathcal{F}_c$ is the feasible region defined by (4b)–(4d), and in the objective function (6a), the ℓ_1-regularization $\sum_{c\in\mathcal{C}} \|\boldsymbol{p}^c - \boldsymbol{p}^0\|_1$ is replaced with a linear term $\sum_{i,c} w_i^c$ and reformulated in constraint (6d).

Let us introduce auxiliary variable $\boldsymbol{p}^{0,c}$ and impose the following constraint:

$$\boldsymbol{p}^{0,c} = \boldsymbol{p}^0, \quad \forall c \in \mathcal{C}.$$

Also notice that, since the objective function has the term $\sum_{i,c} w_i^c$, at the optimum, $\boldsymbol{w}^c = |\boldsymbol{p}^c - \boldsymbol{p}^0|$ must hold. Hence, we can remove the constraints $-\Delta\boldsymbol{p} \le \boldsymbol{p}^c - \boldsymbol{p}^0 \le \Delta\boldsymbol{p}$ and add an upper bound $\boldsymbol{w}^c \le \Delta\boldsymbol{p}$. In this way, the number of constraints is reduced. We have the following reformulation:

$$\min \quad f(\boldsymbol{p}^0) + \tau \sum_{i\in\mathcal{G},c\in\mathcal{C}} w_i^c \tag{7a}$$

$$\text{s.t.} \quad (\boldsymbol{p}^c, \boldsymbol{\theta}^c) \in \mathcal{F}_c \quad \forall c \in \overline{\mathcal{C}} \tag{7b}$$

$$-\boldsymbol{w}^c \le \boldsymbol{p}^c - \boldsymbol{p}^{0,c} \le \boldsymbol{w}^c \quad \forall c \in \mathcal{C} \tag{7c}$$

$$\boldsymbol{w}^c \le \Delta\boldsymbol{p} \quad \forall c \in \mathcal{C} \tag{7d}$$

$$\boldsymbol{p}^{0,c} - \boldsymbol{p}^0 = \boldsymbol{0} \quad \forall c \in \mathcal{C} \tag{7e}$$

which is ready for applying ADMM-based decomposition.

III. Decomposition Algorithms Based on ADMM

Problem (7) is a large-scale optimization problem. However, inspecting the structure of the formulation reveals that the constraints are almost separable into contingencies, except for constraint (7e) which couples the feasible sets of different contingencies. This coupling can be separated by penalizing constraint (7e) and forming the augmented Lagrangian of (7):

$$L_\gamma = f(\boldsymbol{p}^0) + \tau \sum_{i\in\mathcal{G},c\in\mathcal{C}} w_i^c + \sum_{c\in\mathcal{C}} (\boldsymbol{\lambda}^c)^\top \left(\boldsymbol{p}^{0,c} - \boldsymbol{p}^0\right) + \frac{\gamma}{2} \sum_{c\in\mathcal{C}} \|\boldsymbol{p}^{0,c} - \boldsymbol{p}^0\|^2 \tag{8}$$

where $\gamma > 0$ is a penalty parameter.

A. Decomposition by ADMM

Define the primal variables $\boldsymbol{x} = (\boldsymbol{p}^0, \boldsymbol{\theta}^0)$ and $\boldsymbol{z} = (\boldsymbol{z}^c)_{c\in\mathcal{C}}$, where $\boldsymbol{z}^c = (\boldsymbol{p}^c, \boldsymbol{\theta}^c, \boldsymbol{p}^{0,c}, \boldsymbol{w}^c)$, and the dual variable $\boldsymbol{\lambda} = (\boldsymbol{\lambda}^c)_{c\in C}$. The traditional ADMM for solving (7) has the following form [6]:

$$\boldsymbol{x}_{t+1} = \arg\min_{\boldsymbol{x}\in X} L_\gamma(\boldsymbol{x}, \boldsymbol{z}_t, \boldsymbol{\lambda}_t) \tag{9a}$$

$$\boldsymbol{z}_{t+1} = \arg\min_{\boldsymbol{z}\in Z} L_\gamma(\boldsymbol{x}_{t+1}, \boldsymbol{z}, \boldsymbol{\lambda}_t) \tag{9b}$$

$$\boldsymbol{\lambda}_{t+1} = \boldsymbol{\lambda}_t + \gamma\left(\boldsymbol{A}\boldsymbol{x}_{t+1} + \boldsymbol{B}\boldsymbol{z}_{t+1} - \boldsymbol{h}\right) \tag{9c}$$

where $X = \mathcal{F}_0$, the set Z is the feasible region defined by constraints (7b)–(7d), and $\boldsymbol{A}\boldsymbol{x}+\boldsymbol{B}\boldsymbol{z} = \boldsymbol{h}$ represents the coupling constraint (7e).

To facilitate the presentation, define the following two key optimization problems:

$$\min_{(\boldsymbol{p}^0,\boldsymbol{\theta}^0)\in\mathcal{F}_0} f(\boldsymbol{p}^0) - (\boldsymbol{p}^0)^\top\boldsymbol{\alpha} + \frac{\gamma}{2}\sum_{c\in\mathcal{C}} \|\boldsymbol{p}^0 - \boldsymbol{\beta}^c\|^2 \tag{10}$$

and

$$\min_{\boldsymbol{p}^c,\boldsymbol{\theta}^c,\boldsymbol{p}^{0,c},\boldsymbol{w}^c} \quad \tau \boldsymbol{e}^\top \boldsymbol{w}^c + \boldsymbol{\alpha}^\top (\boldsymbol{p}^{0,c} - \boldsymbol{\beta}) + \frac{\gamma}{2}\|\boldsymbol{p}^{0,c} - \boldsymbol{\beta}\|^2 \quad (11)$$
$$\text{s.t.} \quad (\boldsymbol{p}^c, \boldsymbol{\theta}^c) \in \mathcal{F}_c$$
$$-\boldsymbol{w}^c \le \boldsymbol{p}^c - \boldsymbol{p}^{0,c} \le \boldsymbol{w}^c$$
$$\boldsymbol{w}^c \le \Delta \boldsymbol{p}$$

where the parameters $\boldsymbol{\alpha}$, $\boldsymbol{\beta}^c$, and $\boldsymbol{\beta}$ will be specified in the algorithms.

Algorithm 1 applies ADMM (9) to solve the min-impact C-SCOPF (7).

Algorithm 1: ADMM for Min-Impact C-SCOPF

1: **Initialization**: $t = 1$
2: **repeat**
3: **for** $c \in \{0, 1, \ldots, C\}$ **do**
4: **if** $c = 0$ **then**
5: Solve (10) for $\boldsymbol{\alpha} = \sum_{c\in\mathcal{C}} \boldsymbol{\lambda}_t^c$ and $\boldsymbol{\beta}^c = \boldsymbol{p}_t^{0,c}$
6: Denote the optimal solution as $(\boldsymbol{p}_{t+1}^0, \boldsymbol{\theta}_{t+1}^0)$
7: **else**
8: Solve (11) for $\boldsymbol{\alpha} = \boldsymbol{\lambda}_t^c$ and $\boldsymbol{\beta} = \boldsymbol{p}_{t+1}^0$
9: Denote optimal solution as $(\boldsymbol{p}^c, \boldsymbol{\theta}^c, \boldsymbol{p}^{0,c}, \boldsymbol{w}^c)_{t+1}$
10: Update multipliers:

$$\boldsymbol{\lambda}_{t+1}^c = \boldsymbol{\lambda}_t^c + \gamma\left(\boldsymbol{p}_{t+1}^{0,c} - \boldsymbol{p}_{t+1}^0\right)$$

11: **end if**
12: **end for**
13: $t \leftarrow t + 1$
14: **until** a stopping criterion is met.

Notice that, for $c \in \{1, 2, \ldots, C\}$, the subproblems (11) for C contingencies can be solved in parallel. The following theorem shows the convergence of Algorithm 1.

Theorem 1: Assume that $f(\boldsymbol{p}^0)$ is closed, proper, and convex. The ADMM iterates in Algorithm 1 satisfy that as $t \to \infty$, the following hold:

1) $\boldsymbol{p}_t^{0,c} - \boldsymbol{p}_t^0 \to \boldsymbol{0}$ for each $c \in \mathcal{C}$;
2) the objective function value $f(\boldsymbol{p}_t^0) + \tau \sum_{i\in\mathcal{G}, c\in\mathcal{C}} (w_i^c)_t$ converges to the optimal value;
3) the dual variable $\boldsymbol{\lambda}_t^c$ converges to dual optimal solution.

Proof: It suffices to verify that the Lagrangian L_0 defined in (8) with $\gamma = 0$ has a saddle point. Then, we can invoke the convergence theorem of ADMM given in [6, Section 3.2.1]. Equivalently, it suffices to show that the strong duality holds between the primal problem (7) and the following dual problem:

$$\max_{\boldsymbol{\lambda}} \min_{\boldsymbol{x},\boldsymbol{z}} \quad L_0(\boldsymbol{x}, \boldsymbol{z}, \boldsymbol{\lambda})$$
$$\text{s.t.} \quad (7\text{b}), (7\text{c}), (7\text{d}) \quad (12)$$

which in turn is a generalized dual of (7), where only constraint (7e) is dualized. Notice that the feasible region defined by (7b), (7c), and (7d) is bounded. The theory of generalized duality for linear programs guarantees the strong duality property if both (7) and (12) are both feasible, which holds for our case. This finishes the proof. □

B. Accelerated ADMM

The seminal work of Nesterov [34] proposes a general algorithmic framework to significantly accelerate the traditional gradient descent algorithms for solving convex optimization problems. A recent work [23] shows that Nesterov's framework can also accelerate the ADMM algorithm.

In Algorithm 2, we propose the accelerated ADMM algorithm for the SCOPF. The key difference from the traditional ADMM (Algorithm 1) is the additional acceleration step in Lines 12–16 in Algorithm 2 and the two new sequences $\hat{\boldsymbol{p}}_{t+1}^{0,c}$ and $\hat{\boldsymbol{\lambda}}_{t+1}^c$. In particular, the acceleration step is carried out when the largest residual $(\max(d_{t-1}, r_{t-1}) - \max(d_t, r_t))$ has been reduced, where d_t, r_t are defined as

$$r_t = \max_c \left\|\boldsymbol{p}_t^{0,c} - \boldsymbol{p}_t^0\right\|_\infty$$
$$d_t = \max_c \left(\left\|\boldsymbol{p}_t^c - \boldsymbol{p}_{t-1}^c\right\|_\infty, \left\|\boldsymbol{\theta}_t^c - \boldsymbol{\theta}_{t-1}^c\right\|_\infty, \left\|\boldsymbol{p}_t^{0,c} - \boldsymbol{p}_{t-1}^{0,c}\right\|_\infty, \left\|\boldsymbol{w}_t^c - \boldsymbol{w}_{t-1}^c\right\|_\infty\right).$$

Algorithm 2: Accelerated ADMM for Min-Impact C-SCOPF

1: **Initialization**: $t = 1$
2: **repeat**
3: **for** $c \in \{0, 1, \ldots, C\}$ **do**
4: **if** $c = 0$ **then**
5: Solve (10) for $\boldsymbol{\alpha} = \sum_{c\in\mathcal{C}} \hat{\boldsymbol{\lambda}}_t^c$ and $\boldsymbol{\beta}^c = \hat{\boldsymbol{p}}_t^{0,c}$
6: Denote the optimal solution as $(\boldsymbol{p}_{t+1}^0, \boldsymbol{\theta}_{t+1}^0)$
7: **else**
8: Solve (11) for $\boldsymbol{\alpha} = \hat{\boldsymbol{\lambda}}_t^c$ and $\boldsymbol{\beta} = \boldsymbol{p}_{t+1}^0$
9: Denote the optimal solution $(\boldsymbol{p}^c, \boldsymbol{\theta}^c, \boldsymbol{p}^{0,c}, \boldsymbol{w}^c)_{t+1}$
10: Update multipliers:

$$\boldsymbol{\lambda}_{t+1}^c = \hat{\boldsymbol{\lambda}}_t^c + \gamma\left(\boldsymbol{p}_{t+1}^{0,c} - \boldsymbol{p}_{t+1}^0\right)$$

11: Acceleration step:
12: **if** $\max(d_t, r_t) - \max(d_{t+1}, r_{t+1}) > 0$ **then**
13: Update:

$$a_{t+1} = \frac{1 + \sqrt{1 + 4a_t^2}}{2}$$
$$\hat{\boldsymbol{p}}_{t+1}^{0,c} = \boldsymbol{p}_{t+1}^{0,c} + \frac{a_t - 1}{a_{t+1}}\left(\boldsymbol{p}_{t+1}^{0,c} - \boldsymbol{p}_t^{0,c}\right)$$
$$\hat{\boldsymbol{\lambda}}_{t+1}^c = \boldsymbol{\lambda}_{t+1}^c + \frac{a_t - 1}{a_{t+1}}\left(\boldsymbol{\lambda}_{t+1}^c - \boldsymbol{\lambda}_t^c\right)$$

14: **else**
15: Update:

$$a_{t+1} = 1, \quad \hat{\boldsymbol{p}}_{t+1}^{0,c} = \boldsymbol{p}_{t+1}^{0,c}, \quad \hat{\boldsymbol{\lambda}}_{t+1}^c = \boldsymbol{\lambda}_{t+1}^c$$

16: **end if**
17: **end if**
18: **end for**
19: $t \leftarrow t + 1$
20: **until** a stopping criterion is met.

TABLE I
DESCRIPTION OF TEST POWER SYSTEMS. $|\mathcal{N}|$ IS THE NUMBER OF BUSES; $|\mathcal{G}|$ IS THE NUMBER OF GENERATORS; $|\mathcal{B}|$ IS THE NUMBER OF BRANCHES; $|\mathcal{C}|$ IS THE NUMBER OF CONTINGENCIES; AND #VAR IS THE NUMBER OF VARIABLES IN THE PROPOSED FORMULATION (4A)–(4E)

Case	$\lvert\mathcal{N}\rvert$	$\lvert\mathcal{G}\rvert$	$\lvert\mathcal{B}\rvert$	$\lvert\mathcal{C}\rvert$	#Var
NE39	39	10	46	30	2728
IEEE118	118	54	186	130	37990
IEEE300	300	69	411	120	80949
PL2383	2383	320	3572	120	615406
PL3012	3012	293	3572	150	953867

It is shown that Algorithm 2 can accelerate the traditional ADMM (Algorithm 1) to obtain an optimal convergence rate for a first-order method under favorable conditions. For example, when the objective function is strongly convex, Algorithm 2 achieves an ϵ-optimal solution within $O(1/\sqrt{\epsilon})$ iterations, whereas Algorithm 1 needs $O(1/\epsilon)$ iterations [23]. The objective function being strongly convex is a stringent requirement in order to establish this theoretical convergence rate. For the min-impact C-SCOPF model (4), the objective function is not strongly convex. However, computational experiments in Section IV show that Algorithm 2 can considerably reduce the number of iterations.

Nonetheless, let us not overlook the usefulness of Algorithm 1. In fact, Algorithm 1 facilities our understanding of the acceleration. More importantly, it has more robust convergence, e.g., Theorem 1 establishes its convergence under quite general conditions. A closer study in the computation performance also shows that Algorithm 2 needs more dedicate algorithmic setup to fully realize its efficiency. For example, warm-start is more crucial for Algorithm 2. This can be partially explained by the fact that the acceleration step (Lines 12–16) in Algorithm 2 causes jumps in the parameters, which makes subproblems more difficult to solve starting from the solution of the previous iteration. We propose a warm-start strategy which uses other contingency's solution within the same iteration to speed up the subproblems of Algorithm 2 in case of a big jump.

IV. COMPUTATIONAL EXPERIMENTS

A. Experimental Setup

The proposed algorithms are implemented in MATLAB 7.10. All tests are conducted on a 64-bit Windows 7 ThinkPad W520 with Intel i7-2720QM 2.2-GHz CPU and 8 GB of RAM. The power systems used in this section are summarized in Table I and their data are extracted from the software toolbox MATPOWER [41].

A contingency considered in our experiments refers to the failure of a transmission line. Every active generator is able to adjust up to 10% of its maximum power output capacity for the post-contingency actions. The number of contingency scenarios in each system is presented in the fifth column of Table I, and "#Var" is the number of decision variables in the min-impact C-SCOPF model.

We select $\tau = 10^{-3}\sqrt{|\mathcal{G}|}$ in (7a) and $\gamma = 1$ in (10)–(11), and use the following stopping conditions based on the decrease of the primal and dual residuals [6]:

$$r_t \le \epsilon^{abs}\sqrt{|\mathcal{N}||\mathcal{C}|} + \epsilon^{rel}\max\left(\sqrt{\sum_{c\in\mathcal{C}}\|(\boldsymbol{p}^{0,c})_t\|^2}, \sqrt{|\mathcal{C}|}\|(\boldsymbol{p}^0)_t\|\right)$$

$$d_t \le \epsilon^{abs}\sqrt{2|\mathcal{N}|} + \epsilon^{rel}\sqrt{\sum_{c\in\mathcal{C}}\|(\boldsymbol{\lambda}^c)_t\|^2}$$

where $\epsilon^{rel} = 10^{-4}$, $\epsilon^{abs} = 10^{-3}$. We say that a generator i is *rescheduled* for contingency $c \in \mathcal{C}$ if generator i's post-contingency output is sufficiently different from its pre-contingency level, i.e., $|p_i^c - p_i^0| > 10^{-3}$.

B. Models Analysis

In this section, we compare the following models: the traditional P-SCOPF model (1), the traditional C-SCOPF model (2), the traditional C-SCOPF model with integer constraints (3), which we call the MIP model, and the proposed min-impact C-SCOPF model (4).

Here we want to emphasize the differences in the scope and goal of the analysis in this paper from the ones appeared in the literature. In particular, our goal is to study the proposed min-impact SCOPF formulation and algorithms in the context of DC models, whereas the works in [10] and [30] aim to solve AC SCOPF models with limited re-dispatch actions. The DC SCOPF with the MIP formulation (3) is solved as an intermediate step to provide a list of contingencies and re-dispatch generators to the AC SCOPF model [30]. Therefore, it is reasonable to use a small number of allowable re-dispatch actions in this DC SCOPF problem with integer variables, and solve it to a larger optimality gap if needed to speed up the convergence. Also, since contingency filtering techniques are used, the set of contingencies in these works is usually small [10], [30]. However, for our purpose of studying the effectiveness of the min-impact SCOPF, we want to solve all the above formulations with DC models as precisely as possible to have an accurate comparison, and we also test the models on large-scale systems with a large number of contingencies to explore its potential for solving practical problems to optimality. We believe such a comparison constitutes an essential part in a thorough and scientific study of the proposed model and algorithms.

The traditional P-SCOPF and C-SCOPF models are solved using the state-of-the-art interior-point solver SDPT3 called through CVX (see [16] and [36]); the MIP model is solved using Gurobi v5.5.0 with the default setting (e.g., the relative optimality gap is 10^{-4} and the absolute optimality gap is 10^{-10} [24]). To demonstrate the advantage of the ADMM decomposition, the min-impact C-SCOPF is solved by two methods: the interior-point method without decomposition and the accelerated ADMM algorithm. The computation times of these algorithms are shown under the "Time" columns in Table II, with "Time (IPM)" and "Time (Alg 2)" for the two

TABLE II
COMPARISON OF MODELS IN TERMS OF OBJECTIVE VALUES, NUMBER OF CORRECTIVE ACTIONS, AND RUNNING TIMES (IN SECONDS)

		P-SCOPF		C-SCOPF			MIP				Min-Impact			
Case	$\|\mathcal{C}\|$	Cost	Time	%Res	Cost	Time	N_c	%Res	Cost	Time	%Res	Cost	Time (IPM)	Time (Alg 2)
NE39	30	infeas.	-	98.71	564.54	1.19	3	20.64	564.54	1.02	7.41	564.54	2.06	0.52
IEEE118	115	1271.18	3.26	98.16	1261.46	5.61	2	1.80	1262.61	205.37	1.52	1261.51	7.03	0.91
IEEE300	89	infeas.	-	96.71	7115.87	14.00	5	7.23	7115.88	363.21	7.67	7116.56	20.39	1.38
PL2383	36	19134.51	96.04	56.14	18461.95	84.05	9	2.49	18511.24	10995.59	0.87	18461.95	81.32	24.11
PL3012	36	25151.41	184.58	81.95	25058.10	114.43	14	2.05	25063.80	13636.34	2.06	25058.24	121.60	37.04

methods solving the min-impact C-SCOPF model. The running times are reported in seconds.

In all experiments, the same value of N_c is used for every contingency in the MIP model. As the MIP model is solved by a MIP solver, we observe that the running time in general decreases when the number N_c of allowed reschedules increases (see similar observations in [30]). Thus in order to compare the MIP model and our proposed min-impact C-SCOPF model in a fair way, we choose N_c as large as possible so that the levels of average rescheduling percentages of two models are similar and the computation time of the MIP model is minimized.

1) Operational Costs and Minimal Impact Corrections: Comparing the four SCOPF models in Table II, a benefit of the P-SCOPF model is that no post-contingency rescheduling is needed when the system is feasible. However, it may happen that there is no pre-contingency plan feasible for all the contingencies, for example, in the case of NE39 and IEEE300. Also, the P-SCOPF model incurs in general a higher generation cost for the normal case. As shown in the IEEE118, PL2382, and the PL3012 cases, the normal state operational costs (column "Cost") of P-SCOPF are on average 1.55% higher than the corrective SCOPF models.

If we compare the traditional C-SCOPF with the min-impact C-SCOPF in Table II, we can see that the number of rescheduling is significantly reduced in the min-impact C-SCOPF model, i.e., %Res is much smaller for the min-impact model. For all five test systems, the min-impact C-SCOPF requires less than 8% of the generators to be rescheduled, and for the large power systems (PL2383 and PL3012), only 0.87% and 2.06% of all generators need to reschedule for any contingency. In comparison, the traditional C-SCOPF requires almost all generators to be rescheduled for NE39, IEEE118, and IEEE300, 56.14% rescheduling for the 2383-bus system, and 81.95% for the 3012-bus system. At the same time, the operational costs of C-SCOPF and min-impact C-SCOPF are essentially the same for all practical purposes. It shows that the small number of reschedules from the ℓ_1-regularization model increases the power system reliability without increasing the operation cost.

Table III reports the average absolute value of MW rescheduled between the normal case solution and a post-contingency corrective action. It shows that the proposed min-impact C-SCOPF model requires a significantly less amount of MW rescheduling than the traditional C-SCOPF and the MIP models in all test cases. In particular, comparing to the MIP model, the min-impact C-SCOPF model reduces the amount of MW rescheduling by 80.77% for NE39, 97.22% for IEEE118, 96.06% for IEEE300, 89.59% for PL2383, and 47.44% for PL3012. Comparing to the traditional C-SCOPF, the amount of MW rescheduling is reduced even more: 90.88% for NE39, 99.85% for IEEE118, 97.83% for IEEE300, 95.84% for PL2328, and 93.26% for PL3012. It is clear that ℓ_1-regularization not only produces a sparse solution, but also substantially reduces the total amount of MW rescheduling.

TABLE III
COMPARISON OF AVERAGE RESCHEDULED MW

		MW Rescheduled		
Case	Demand	C-SCOPF	MIP	Min-Impact
NE39	6254.2	297.1	140.9	27.1
IEEE118	4242.0	410.8	21.6	0.6
IEEE300	23525.8	741.6	408.2	16.1
PL2383	24548.2	1296.7	517.9	53.9
PL3012	27169.6	1184.4	151.8	79.8

TABLE IV
SOLUTIONS OF THE TRADITIONAL C-SCOPF MODEL FOR NE39

$\mathcal{G}$	Normal	Cont. 1	Cont. 2	Cont. 3	Cont. 4	Cont. 5
G1	83.2	**158.0**	**148.4**	**151.0**	**166.4**	**159.6**
G2	646.0	**638.8**	**628.5**	**629.2**	646.0	**638.0**
G3	636.1	**601.2**	**666.7**	**667.5**	**578.1**	**685.5**
G4	648.4	**635.5**	**631.8**	**631.7**	**630.7**	**643.7**
G5	508.0	**493.6**	**491.2**	**491.2**	**490.6**	**499.8**
G6	642.9	**662.8**	**655.1**	**655.0**	**653.0**	**587.9**
G7	580.0	**564.7**	**561.8**	**561.8**	**560.4**	**533.6**
G8	564.0	**553.6**	**545.9**	**543.8**	**564.0**	**555.7**
G9	865.0	**853.3**	**843.1**	**839.1**	865.0	**857.2**
G10	1080.7	**1093.1**	**1081.7**	**1083.9**	**1100.0**	**1093.2**

TABLE V
SOLUTIONS OF THE MIN-IMPACT C-SCOPF MODEL FOR NE39

$\mathcal{G}$	Normal	Cont. 1	Cont. 2	Cont. 3	Cont. 4	Cont. 5
G1	83.2	**95.4**	83.2	**96.0**	**123.5**	83.2
G2	646.0	646.0	646.0	646.0	646.0	646.0
G3	624.9	**604.1**	624.9	**600.0**	**576.0**	624.9
G4	650.8	650.8	650.8	**651.4**	650.8	650.8
G5	508.0	508.0	508.0	508.0	508.0	508.0
G6	640.8	640.8	640.8	**648.9**	640.8	640.8
G7	580.0	580.0	580.0	580.0	580.0	580.0
G8	564.0	564.0	564.0	564.0	564.0	564.0
G9	865.0	865.0	865.0	865.0	865.0	865.0
G10	1055.0	**1100.0**	1055.0	**1095.1**	**1100.0**	1055.0

We use the NE39 test case to further illustrate the effect of the min-impact C-SCOPF model on reducing the number of reschedulings. Tables IV and V show the solutions of the traditional C-SCOPF and the min-impact C-SCOPF models, respectively. There are 10 generators and 30 transmission contingencies in the NE39 system. To save space, we only show 5 contingencies.

For the traditional C-SCOPF model in Table IV, almost all generators have to be rescheduled to respond to the contingencies (indicated by numbers in bold face), whereas the min-impact C-SCOPF model is able to reschedule a small percentage of

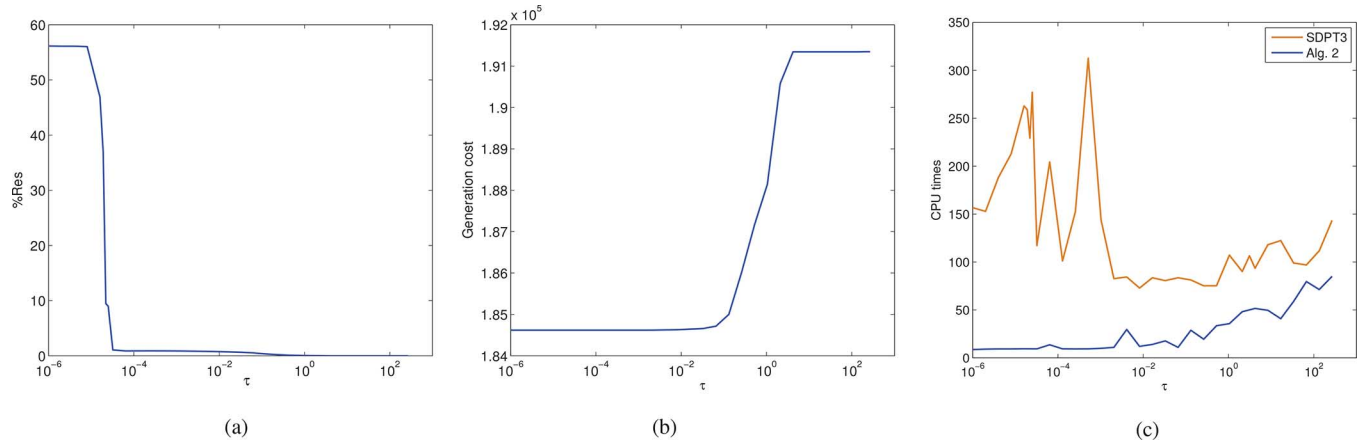

Fig. 1. Sparsity level, generation cost, and CPU times as functions of τ. (a) Percentage of rescheduled generators %Res. (b) Generation cost. (c) CPU times.

all generators. For example, In contingencies 1 and 5, all generators have to reschedule in the traditional C-SCOPF model, while only 3 out of 10 generators need to reschedule for the min-impact C-SCOPF model for contingency 1 and no rescheduling for contingency 5.

2) Computation Time: Let us go back to Table II. If we compare the running times of solving the MIP model and those of solving the min-impact C-SCOPF model without decomposition (column "Time (IPM)"), we can see that, to achieve a similar level of average rescheduling percentages ("%Res"), the min-impact C-SCOPF model without decomposition can already be solved much faster than the MIP model. In particular, for the small system NE39, the min-impact C-SCOPF is slightly slower, but for the medium-size systems (118-bus and 300-bus), the solution time of the min-impact C-SCOPF is on average 4.45% of the MIP model; for the large systems (2383-bus and 3012-bus), on average the min-impact C-SCOPF can be solved within or around 2 minutes, whereas the MIP model needs more than 3 hours. Also, the operational costs of the min-impact C-SCOPF model are slightly better than the MIP model for most test cases.

The last column ["Time (Alg.2)"] shows the running times of solving the min-impact C-SCOPF models with the accelerated ADMM decomposition Algorithm 2. Comparing to the running times without decomposition ["Time (IPM)"], we can see that the decomposition method is effective in reducing the computation times from the direct method. For the two large systems, Algorithm 2's solution time is on average 30.05% of that of the interior-point solver. Later, we will show more detailed study of the Algorithm 2's performance.

3) Selection of Regularization Parameter: It is a non-trivial task to select an appropriate value for the parameter τ in the min-impact C-SCOPF model (4). In general, higher values of τ increase the weight of the ℓ_1-regularization term in (4a), therefore, increase the sparsification effect.

We use the PL2383 system as an example to illustrate the impact of τ on the sparsity of the solution, the operational cost, and the computation time. Similar observations apply to other test cases. In particular, Fig. 1(a) plots the average percentage of the number of generation rescheduling ("%Res") in the min-impact C-SCOPF model as a function of τ. We can see that there is a "phase-transition" type behavior, for all values of $\tau \geq 3.2 \times 10^{-5}$, the min-impact model produces consistently low number of rescheduling around 1% or lower.

Fig. 1(b) shows the plot of operational cost versus τ. The operational cost of the min-impact C-SCOPF model is essentially the same as that of the traditional C-SCOPF for all values of $\tau \leq 0.065$, and then increases to the level of the P-SCOPF model for all $\tau \geq 2.0$. Therefore, there is a range of $\tau \in [3.2 \times 10^{-5}, 0.065]$, where the min-impact C-SCOPF model generates a pre-contingency plan that requires very few post-contingency actions and at the same time keeps essentially the same cost level as the traditional corrective model.

Fig. 1(c) reports the CPU times in seconds of the interior-point solver and the ADMM Algorithm 2. The running times for the accelerated ADMM remain almost constant in the range of $\tau \leq 10^{-1}$ and then moderately increase as τ becomes larger, but is always smaller than the interior-point solver.

C. Tests for Large Number of Contingencies

This section illustrates the computational performance of proposed algorithms in solving the min-impact C-SCOPF model with a large number of contingencies, where the MIP model with traditional DC C-SCOPF and integer constraints (3) is prohibitive to solve to optimality due to computational complexity.

1) Warm-Start Strategy: As discussed in Section III-B, the accelerated ADMM needs a more dedicate warm-start to speed up the subproblems. The usual strategy of using the previous iteration's solution as the starting point is not effective in some cases, especially due to the acceleration steps that introduce jumps in the parameters $\hat{\boldsymbol{\lambda}}$. To overcome this issue, we propose to use a solution of another contingency in the same iteration t as the warm-start for a given contingency. First, we use the previous step's solution strategy for solving a few contingencies to predict the jump. If a significant increase in running time is observed, we switch to this warm-start technique. The simple strategy proves to be quite effective in speeding up the subproblems.

2) Computation Time: We solve the min-impact C-SCOPF model (7) using the two ADMM-base decomposition methods (columns "Alg. 1" and "Alg. 2" in Table VI) and the interior-point method by SDPT3 (column "IPM"). Column $|\mathcal{C}|$ shows

TABLE VI
COMPARISON OF RUNNING TIMES (IN SECONDS)

			IPM	Alg. 1		Alg. 2	
Case	$\|\mathcal{C}\|$	%Res	Time	Iter	Time	Iter	Time
NE39	30	7.41	2.06	189	0.74	113	0.52
IEEE118	130	1.37	9.25	183	2.31	60	0.99
IEEE300	120	7.24	22.40	228	7.25	35	2.61
PL2383	120	0.15	269.90	114	122.68	46	112.49
PL3012	150	0.98	397.94	129	233.75	48	171.86

a larger number of contingencies for each test case comparing to Table II, "%Res" is the average percentage of the number of rescheduled generators achieved by the min-impact C-SCOPF model, and "Iter" is the number of iterations of the ADMM algorithms. Times are reported in seconds.

The table shows that both Algorithms 1 and 2 clearly outperform the interior-point solver in computation time for all test cases. The accelerated ADMM, i.e., Algorithm 2, requires a fewer number of iterations than the regular ADMM (Algorithm 1), the computation times of Algorithm 2 are also faster than those of Algorithm 1.

It is important to point out that the subproblems for all contingencies in the ADMM-based algorithms can be fully parallelized. In our current implementation such parallelization property has not been exploited, i.e., the algorithms are implemented in a serial fashion in MATLAB, and the CPU times reported in Table VI are the total running times of the serial implementation. We expect that the running times of the ADMM-based algorithms can be substantially reduced in a parallel implementation.

We can see that the min-impact C-SCOPF model is particularly effective for large-scale systems. This can be clearly seen from the last two test systems in Table VI: on average only 0.15% of generators need to be rescheduled for the 2383-bus case with 120 contingencies, and 0.98% of generators rescheduled for the 3012-bus case with 150 contingencies. Comparing to Table II, the rescheduling is 0.87% and 2.06% for the same two test systems but a fewer number of contingencies (36 contingencies), respectively.

V. CONCLUSION

In this paper, we propose a new model for the security-constrained optimal power flow problem with DC power flow constraints, which produces a generation schedule with a minimal number of post-contingency corrections as well as a minimal amount of total MW rescheduled. That is, the new SCOPF model effectively clears contingencies with corrective actions that have a minimal impact on system operations. To achieve this, we apply the ℓ_1-regularization technique to the corrective SCOPF model. We also propose two ADMM-based parallelizable algorithms and warm-start techniques for solving the new model. Computational results comparing with the traditional SCOPF corrective model show that the min-impact C-SCOPF model significantly reduces the number of post-contingency generator rescheduling and the total MW rescheduled. This effect of clearing contingencies with a minimal impact on system operation is particularly clear for large-scale test systems with a large number of contingencies. The min-impact C-SCOPF model achieves essentially the same level of low generation cost as the traditional corrective SCOPF model, and can be solved much faster than the existing SCOPF model with MIP formulation. The proposed ADMM-based algorithms also show promising computational performance comparing to the state-of-the-art interior-point solver in terms of solution speed. These proposed algorithms are viable for parallelization which will further improve the computation time, especially for large-scale power systems.

ACKNOWLEDGMENT

The authors would like to thank the associate editor and the anonymous reviewers for their valuable comments.

REFERENCES

[1] O. Alsac, J. Bright, M. Prais, and B. Stott, "Further developments in LP-based optimal power flow," *IEEE Trans. Power Syst.*, vol. 5, no. 3, pp. 697–711, Aug. 1990.
[2] O. Alsac and B. Stott, "Optimal load flow with steady state security," *IEEE Trans. Power App. Syst.*, vol. PAS-93, no. 3, pp. 745–751, 1974.
[3] A. Ardakani and F. Bouffard, "Identification of umbrella constraints in DC-based security-constrained optimal power flow," *IEEE Trans. Power Syst.*, vol. 28, no. 4, pp. 3924–3934, Nov. 2013.
[4] A. Beck and M. Teboulle, "A fast iterative shrinkage-thresholding algorithm for linear inverse problems," *SIAM J. Imag. Sci.*, vol. 2, no. 1, pp. 183–202, 2009.
[5] F. Bouffard, F. D. Galiana, and J. M. Arroyo, "Umbrella contingencies in security constrained optimal power flow," in *Proc. 15th Power Systems Computation Conf. (PSCC 05)*, Liège, Belgium, Aug. 2005.
[6] S. Boyd, N. Parikh, E. Chu, B. Peleato, and J. Eckstein, "Distributed optimization and statistical learning via the alternating direction method of multipliers," *Found. Trends Mach. Learn.*, no. 3, pp. 1–124, 2011.
[7] E. J. Candés and M. B. Watkin, "An introduction to compressive sampling," *IEEE Signal Process. Mag.*, vol. 25, no. 2, pp. 21–30, Mar. 2008.
[8] F. Capitanescu, M. Glavic, D. Ernst, and L. Wehenkel, "Contingency filtering techniques for preventive security-constrained optimal power flow," *IEEE Trans. Power Syst.*, vol. 22, no. 4, pp. 1690–1697, Nov. 2007.
[9] F. Capitanescu, J. L. M. Ramos, P. Panciatici, D. Kirschen, A. M. Marcolini, P. Platbrood, and L. Wehenkel, "State-of-the-art, challenges, and future trends in security constrained optimal power flow," *Elect. Power Syst. Res.*, vol. 81, no. 8, pp. 1731–1741, 2011.
[10] F. Capitanescu, W. Rosehart, and L. Wehenkel, "Optimal power flow computations with constraints limiting the number of control actions," in *Proc. IEEE Bucharest Power Tech Conf.*, Bucharest, Romania, Jun. 28–Jul. 2, 2009.
[11] F. Capitanescu and L. Wehenkel, "A new iterative approach to the corrective security-constrained optimal power flow problem," *IEEE Trans. Power Syst.*, vol. 23, no. 4, pp. 1533–1541, Nov. 2008.
[12] F. Capitanescu and L. Wehenkel, "Optimal power flow computations with a limited number of controls allowed to move," *IEEE Trans. Power Syst.*, vol. 25, no. 1, pp. 586–587, Feb. 2010.
[13] F. Capitanescu and L. Wehenkel, "Re-dispatching active and reactive powers using a limited number of control actions," *IEEE Trans. Power Syst.*, vol. 26, no. 3, pp. 1221–1230, Aug. 2011.
[14] B. Carlson, Y. Chen, M. Hong, R. Jones, K. Larson, X. Ma, P. Nieuwesteeg, H. Song, K. Sperry, M. Tackett, D. Taylor, J. Wan, and E. Zak, "MISO unlocks billions in savings through the application of operations research for energy and ancillary services markets," *Interfaces*, vol. 42, no. 1, pp. 58–73, Jan. 2012.
[15] N. Chiang, "Structure-exploiting interior point methods for security constrained optimal power flow problems," Ph.D. dissertation, Univ. Edinburgh, Edinburgh, U.K., Apr. 2013.
[16] CVX Research, Inc., CVX: Matlab Software for Disciplined Convex Programming, Version 2.0, Aug. 2012 [Online]. Available: http://cvxr.com/cvx
[17] D. L. Donoho, "Compressed sensing," *IEEE Trans. Inf. Theory*, vol. 52, no. 4, pp. 1289–1306, 2006.
[18] D. L. Donoho and M. Elad, "Optimally sparse representation in general (nonorthogonal) dictionaries via ℓ^1 minimization," *Proc. Nat. Acad. Sci. USA*, vol. 100, no. 5, pp. 2197–2202, 2002.
[19] , Y. C. Eldar and G. Kutyniok, Eds., *Compressed Sensing: Theory and Applications*. Cambridge, U.K.: Cambridge Univ. Press, 2012.

[20] D. Ernst, D. Ruiz-Vega, M. Pavella, P. M. Hirsch, and D. Sobajic, "A unified approach to transient stability contingency filtering, ranking and assessment," *IEEE Trans. Power Syst.*, vol. 16, no. 3, pp. 435–443, Aug. 2001.
[21] FERC Staff, Recent ISO Software Enhancements and Future Software and Modeling Plans, 2011 [Online]. Available: http://www.ferc.gov/industries/electric/indus-act/rto/rto-iso-soft-2011.pdf
[22] Y. Fu, M. Shahidehpour, and Z. Li, "AC contingency dispatch based on security-constrained unit commitment," *IEEE Trans. Power Syst.*, vol. 21, no. 2, pp. 897–908, May 2006.
[23] T. Goldstein, B. O'Donoghue, and S. Setzer, Fast Alternating Direction Optimization Methods, UCLA, Tech. Rep. CAM 12-35, May 2012.
[24] Gurobi Optimization Inc., Gurobi Optimizer Reference Manual, 2013 [Online]. Available: http://www.gurobi.com
[25] R. Jabr, N. Martins, B. Pal, and S. Karaki, "Contingency constrained VAr planning using penalty successive conic programming," *IEEE Trans. Power Syst.*, vol. 27, no. 1, pp. 545–553, Feb. 2012.
[26] K. Karoui, H. Crisciu, A. Szekut, and M. Stubbe, "Large scale security constrained optimal power flow," in *Proc. 16th Power System Computation Conf.*, Glasgow, U.K., 2008.
[27] N. Kumar, P. M. Besuner, S. A. Lefton, D. D. Agan, and D. D. Hilleman, Power Plant Cycling Costs, National Renewable Energy Lab., Tech. Rep., Apr. 2012.
[28] H. Lee, A. Battle, R. Raina, and A. Y. Ng, "Efficient sparse coding algorithms," *Adv. Neural Inf. Process. Syst.*, vol. 19, pp. 801–808, 2007.
[29] Y. Li and J. D. McCalley, "Decomposed SCOPF for improving efficiency," *IEEE Trans. Power Syst.*, vol. 24, no. 1, pp. 494–495, Feb. 2009.
[30] A. Marano-Marcolini, F. Capitanescu, J. Martinez-Ramos, and L. Wehenkel, "Exploiting the use of DC SCOPF approximation to improve iterative AC SCOPF algorithms," *IEEE Trans. Power Syst.*, vol. 27, no. 3, pp. 1459–1466, Aug. 2012.
[31] J. Martinez-Crespo, J. Usaola, and J. L. Fernandez, "Security-constrained optimal generation scheduling in large-scale power systems," *IEEE Trans. Power Syst.*, vol. 21, no. 1, pp. 321–332, Feb. 2006.
[32] A. Monticelli, M. V. F. Pereira, and S. Granville, "Security-constrained optimal power flow with post-contingency corrective rescheduling," *IEEE Trans. Power Syst.*, vol. 2, no. 1, pp. 175–180, Feb. 1987.
[33] B. K. Natarajan, "Sparse approximation solutions to linear systems," *SIAM J. Comput.*, vol. 24, no. 2, pp. 227–234, 1995.
[34] Y. Nesterov, "A method of solving a convex programming problem with convergence rate $O(1/k^2)$," *Soviet Math. Dokl.*, vol. 27, no. 2, pp. 372–276, 1983.
[35] D. Phan and J. Kalagnanam, "Some efficient optimization methods for solving the security-constrained optimal power flow problem," *IEEE Trans. Power Syst.*, vol. 29, no. 2, pp. 863–872, Mar. 2014.
[36] K. C. Toh, M. J. Todd, and R. H. Tutuncu, "A Matlab software package for semidefinite programming," *Optimiz. Meth. Softw.*, vol. 11, pp. 545–581, 1999.
[37] E. Vaahedi, Y. Mansour, C. Fuchs, S. Granville, M. de Lujan Latore, and H. Hamadanizadeh, "Dynamic security constrained optimal power flow/VAR planning," *IEEE Trans. Power Syst.*, vol. 16, no. 1, pp. 38–43, Feb. 2001.
[38] Q. Wang, J. D. McCalley, T. Zheng, and E. Litvinov, "A computational strategy to solve preventive risk-based security-constrained OPF," *IEEE Trans. Power Syst.*, vol. 28, no. 2, pp. 1666–1675, May 2013.
[39] S. J. Wright, R. D. Nowak, and M. A. T. Figueiredo, "Sparse reconstruction by separable approximation," *IEEE Trans. Signal Process.*, vol. 57, no. 7, pp. 2479–2493, Jul. 2009.
[40] P. Yumbla, J. M. Ramirez, and C. Coello, "Optimal power flow subject to security constraints solved with a particle swarm optimizer," *IEEE Trans. Power Syst.*, vol. 23, no. 1, pp. 33–40, Feb. 2008.
[41] R. D. Zimmerman and C. E. Murillo-Sánchez, MATPOWER 4.1 User's Manual, 2011 [Online]. Available: http://www.pserc.cornell.edu/matpower/

Dzung T. Phan received the B.S. degree in mathematics from Vietnam National University, the M.S. degree in computational engineering from the National University of Singapore, and the Ph.D. degree in mathematics from the University of Florida, Gainesville, FL, USA.

He is a Research Staff Member of Mathematical Sciences Department at IBM T. J. Watson Research Center, Yorktown Heights, NY, USA. His research interests lie in the field of the optimization theory and algorithms including methods for problems arising from power systems.

Xu Andy Sun (S'10–M'12) received the B.S. degree in electronic engineering from Tsinghua University, Beijing, China, and the Ph.D. degree in operations research from the Massachusetts Institute of Technology, Cambridge, MA, USA.

He held a postdoctoral position at the IBM T. J. Watson Research Center, Yorktown Heights, NY, USA. He is currently an Assistant Professor at the H. Milton Stewart School of Industrial and Systems Engineering of the Georgia Institute of Technology, Atlanta, GA, USA. His main research interests are in robust and stochastic optimization and large-scale computational problems in power systems. He has worked with the ISO New England (ISO-NE) on the robust unit commitment problem.